Received July 22, 2018, accepted September 2, 2018, date of publication September 13, 2018, date of current version October 12, 2018.

*Digital Object Identifier 10.1109/ACCESS.2018.2869878*

# Design and Performance Evaluation for a Non-Line of Sight VLC Dimmable System Based on SC-LPPM

**NAZMI A. MOHAMMED[1,2] AND KAREEM A. BADAWI[1,3]**

[1]Photonic Research Lab, College of Engineering, Shaqra University, Riyadh 11961, Saudi Arabia
[2]Electronics and Communication Engineering Department, Obour Institutes, Obour City 11828, Egypt
[3]Electronics and Communication Engineering Department, Higher Technological Institute, Cairo 44635, Egypt

Corresponding author: Nazmi A. Mohammed (nazzazzz@gmail.com)

**ABSTRACT** This work explores the performance of a distinct power saving and relatively simple design visible light communication system based on pulse position modulation (PPM) modulation scheme in a real life (i.e. diffuse) scenario. The mathematical background for both communication and illumination performance is developed for the Sub-Carrier Pulse Position Modulation (SC-LPPM) Scheme in non-line-of-sight (NLOS) environment. An evaluative study is then carried out to provide an integrated picture for the SC-LPPM performance under several system/environmental parameters. Adding the NLOS components increases the total received power, but still, the LOS component dominates. At the corners of a typical room, the received optical power enhances by 120% when including NLOS components, while at room center the optical power enhances only by 12%. For illumination, the NLOS components improve the system's lighting performance and ensure meeting illumination standards. It provides an extra illumination of about 260 lux at room corner and 175 lux at room center over LOS scenario. Wall reflectivity ($\rho$), subcarrier modulation factor (SCMF), and the number of time slots (L) are environmental/system parameters that can significantly optimize the overall performance. For diffuse scenario, a BER of $10^{-5}$ to $10^{-7}$ with $L = 4$, normal wall reflectivity (plaster walls $\rho = 0.8$) and 100% SCMF (i.e. 20 mW/LED) can be achieved easily at bit rates of 1 to 2 Mbps. These BER performance levels can be enhanced by selecting wall painting/ materials with high reflectivity. As a power saving scheme, increasing SCMF with low power/LED level can greatly enhance the BER performance in the diffuse scenario. A remarkable BER performance of $10^{-9}$ can be reached when increasing SCMF by 25% (i.e. to reach 25 mW/LED) under the same conditions ($L = 4$, $\rho = 0.8$ and 1–2 Mbps). At higher data rates the performance is getting worse but still can be optimized, controlled, and enhanced through using a careful choice of environmental and system parameters that can be selected from this work.

**INDEX TERMS** Bit error rate, illumination, non-line of sight, sub-carrier pulse position modulation, visible light communication.

## I. INTRODUCTION

Recently, visible light communication (VLC) gained a growing interest in research and development at a global level as a supplement to radio frequency (RF) technology [1], [2]. VLC technology offers many advantages over (RF) technology such as free license bandwidth (BW), no interference with surrounding electronic & RF circuits, an available infrastructure, privacy and security [3].

VLC using white light-emitting-diodes (LEDs) has attracted considerable attention and has become a valuable method for wireless communication. Compared with the existing incandescent, LEDs offer the advantages of longer lifetimes, smaller sizes, faster switching rate, and much higher durability and reliability. Taking advantage of their faster switching rate, white LEDs can be used for visible light communication (VLC) [4], [5].

VLC is used in various applications, including localization, high bit-rate data broadcasting within homes and offices, high speed video streaming, electromagnetic interference (EMI) sensitive environments like aircraft, traffic control systems, and underwater data transmission [6]–[8].

An interesting research area regarding VLC data broadcasting within homes and offices is effectively satisfying lighting and communication requirements [5].

  

Controlling lighting levels (i.e. dimming control) while sustaining communication link, are achieved by using different modulation techniques.

Such goals can be met by modulation techniques developed for intensity modulation and direct detection (IM/DD) optical wireless communication (OWC) systems. Such techniques are known as single carrier modulation (SCM) techniques. However, not all of these techniques can meet such goals.

Modulation techniques that meet dimming and communication requirements differ from indoor IR communication [5], this work will be dedicated for VLC scenario only. Efficient dimming performance for VLC system is achieved by using pulse width modulation (PWM) and pulse amplitude modulation (PAM) [9], where data transmission (i.e. communication) is achieved effectively by using on-off keying (OOK) [10] and various types of pulse position modulation (PPM) [11], [12]. Therefore, achieving a stable VLC communication link with efficient dimming control is the main objective for VLC based system and the reason for designing several modulation schemes. Design aspects to achieve previous objectives include: 1) reduction of power consumption, 2) enhanced throughput, 3) higher operating data rates, 4) spectral efficiency, 5) complexity reduction, 6) range and levels of dimming control, and 7) flicker free operation.

It is noteworthy to mention that, at lower to moderate operating system rates, SCM techniques such as OOK, PWM, PAM, and PPM, are considered as straightforward techniques that can be used for implementing a VLC system. However, SCM techniques suffer from the effect of inter symbol interference (ISI) at higher operating bitrates. Hence, equalization techniques such as frequency domain equalizers (FDE), linear feed forward equalizer (FFE), optimum maximum likelihood sequence detection (MLSD), and nonlinear decision feedback equalizers (DFE) [13]–[15], are introduced as a suitable solution to enhance the system performance at higher bitrates. But, due to the high complexity of such process, multicarrier modulation (MCM) techniques such as orthogonal frequency division multiplexing (OFDM) are introduced and compared with previous techniques.

Although MCM techniques showed promising performance at higher operating data rates, they have a high system complexity compared with SCM techniques. Yet it can be predicted that the ISI limitation for the SCM techniques and the equalization techniques complexity will be decreased and enhanced in the future. This study is limited to SCM techniques, equalization techniques and MCM modulation techniques are not considered in this paper.

Literatures presented several PPM based schemes to meet one or more of the previous aspects. Overlapping pulse position modulation (OPPM) [16], multi pulse PPM (MPPM) [17], [18], overlapping MPPM (OMPPM) [19], [20], differential PPM (DPPM) [21], expurgated PPM (EPPM) [22], [23], Multi-level EPPM (MEPPM) [24] and variable PPM (VPPM) [25] are nominated examples.

Recently, sub-carrier pulse position modulation (SC-LPPM) scheme is introduced in [5] and it has the distinct advantage of reducing the total LED power consumption while maintaining both efficient communication (i.e. acceptable data rates and spectral efficiency) and illumination performance [26]. Simple design is an extra advantage [5].

Previous literature that utilize LOS SC-LPPM based VLC system suffer from the absence of BER analysis. This analysis becomes more significant when merged with exploring the effect of different system and environmental parameters.

Another substantial limitation for a more practical evaluation of this scheme is assuming a LOS component only for simple analysis and realization [5], [27]. For a more practical model, it must be taken into consideration that a portion of light is reflected from different surfaces/objects, which can dramatically change the performance of a VLC system. Hence, in addition to the line-of-sight (LOS) communication, a Non-Line-of-Sight (NLOS) (i.e. diffuse reflections) communication exists between the Tx and Rx that should be considered [10], [28]. Once more, a huge shortage in BER analysis can be also observed for this scheme under NLOS Scenario.

In this work, a novel NLOS SC-LPPM technique is explored, evaluated and compared to LOS scenario. This is critical for evaluating the effect of real life operating scenario (i.e. NLOS) on the performance of this scheme, especially for communication and illumination performance. After that, the effect of different VLC system and environmental parameters on the BER performance for both LOS/NLOS SC-LPPM scenarios are introduced and compared. Modulation factor and level that characterized SC-LPPM are addressed and their effect on BER performance is investigated during both LOS/NLOS scenarios.

In the presented work, the system environment and a detailed mathematical background for LOS/NLOS SC-LPPM based VLC system including BER model is presented in section II. Section III contains a detailed discussion for the LOS/NLOS SC-LPPM based VLC system performance. Finally, a conclusion for the obtained results is presented in section IV.

## II. LOS/NLOS SYSTEM MODEL, DESIGN, PARAMETERS, AND SPECIFICATIONS

### A. SYSTEM ENVIRONMENT

In this work, a distinct lighting system where multiple reflections between the room walls, ceiling, and floor are assumed to simulate and evaluate a LOS/NLOS VLC system performance. The system design consists of $i$ identical LED lamps which are equally spaced on the celling of a room at a center position (1.25, 1.25, 2.5), (1.25, 3.75, 2.5), (3.75, 1.25, 2.5), (3.75, 3.75, 2.5). While the receiver is assumed to be at desk level 0.85 m, as shown in Fig. 1. These coordinated and the parameters which will be presented in section II-D, will be used to evaluate the proposed system in section III.

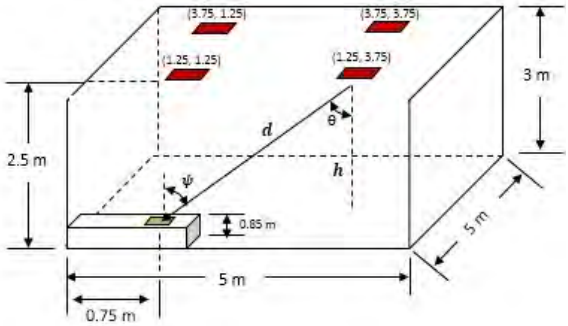


**FIGURE 1.** Room configuration.

The reason for choosing such locations for the LED lamps, is to apply a distinct lighting system that is commonly used in many literatures [5], [6]. Moreover, they will provide acceptable performance as it will be shown in section III.

As indicated in [5] a DC component and a subcarrier component (SC) are the main components required to construct the SC-LPPM waveform. Equal time slots ($L$) can form a symbol interval ($T$) as follows $Ts = T/L$ Each ($L$) can carry an optical data and corresponds to $\log_2 L$ data bits while the rest ($L-1$) have a constant amplitude. While the position of the subcarrier corresponds to its decimal value. Fig.2 shows the waveform of an SC-4PPM Scheme; while (c– a) is the amplitude of the optical signal [27], and (b) is the amplitude of the DC component.

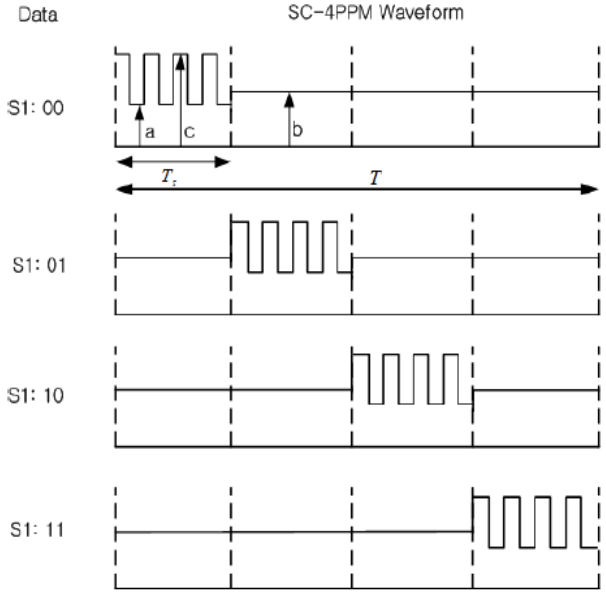


**FIGURE 2.** SC-4 PPM waveform [5].

### B. LOS CHANNEL MODEL

#### 1) COMMUNICATION

The signal strength in an optical communication link is determined by the transmitted optical power, which is irradiated by the LED [5]. To calculate the signal strength of an SC-LPPM signal, only the transmitted power through the subcarrier component is considered, where $P_i^t$ is the optical transmitted power from the $i^{\text{th}}$ LED, $P_{max}^t$ is the maximum optical transmitted power by the LED,

$$P_i^t = M \times P_{max}^t \tag{1}$$

While the optical power factor or subcarrier modulation factor, SCMF, or simply $M$, for a SC-LPPM waveform can be formulated as.

$$SCMF = c - a \tag{2}$$

For a wireless optical channel, the optical power received by the PD can be derived as follows [5], where $P_j^r$ is the optical power received at workplace $j$, and $H(0)$ is the channel response.

$$P_j^r = \sum_{i=1}^{I} \left( H(0) \times P_i^t \right) \tag{3}$$

The channel response for a LOS channel can be obtained using [5], where $A_{eff}$ is the effective area of the PD, $T_s(\theta)$ is the optical filter gain, $g(\theta)$ is the concentrator gain, $\theta$ is the angle of irradiance, and $\psi$ is the angle of incidence.

$$H(0) = \frac{A_{eff}(m+1)}{2\pi d_o^2} T_s(\theta)\, g(\theta) \cos^m \theta \cos \psi \tag{4}$$

Using Eqs. (1), (3), and (4), the total received optical power can be represented as follows, where FOV is the receiver field of view.

$$P_j^r = \begin{cases} (c_i - a_i) \times P_{max}^t \times \dfrac{A_{eff}(m+1)}{2\pi d_o^2} T_s(\theta)\, g(\theta) \\ \quad \cos^m \theta \cos \psi, \quad \theta \le FOV \\ 0, \quad \theta > FOV. \end{cases} \tag{5}$$

The bit error rate (BER) is a main parameter used for evaluating the performance of a communication system. For a SC-LPPM, it can be obtained as [5], where $R_b$ is the bit rate, $N_o$ is the power spectral density of additive white Gaussian noise channel.

$$BER = \frac{L/2}{L-1} Q\left( \frac{1}{2} \sqrt{\frac{3A_{eff}^2 L \left(P_j^r\right)^2 log_2 L}{N_o R_b}} \right) \tag{6}$$

The received optical power $P_j^r$ should be greater than or equal to the minimum power required $P_{req}$, for the SC-LPPM to achieve a given BER which is given by [5].

$$P_{req} = \frac{2}{A_{eff}} Q^{-1}\left( \left( \frac{L-1}{L/2} \right) \times BER \right) \sqrt{\frac{N_o R_b}{3L log_2 L}} \tag{7}$$

#### 2) ILLUMINATION

The output luminous flux generated by a LED lamp can be calculated as indicated in [5], where $i$ is the lamp index and $\varphi_{max}$ is the maximum luminous flux generated by each LED. It is generated when the input waveform has a DC component with maximum amplitude.

$$\varphi_i = N \times \varphi_{max} \tag{8}$$

The brightness factor, N, can be obtained through [5], where $\tau_1$ and $\tau_2$ are $T_S/2$ and $3T_S$, respectively.

$$N = \frac{(\tau_1 \times (a + c) + \tau_2 \times b)}{T}. \tag{9}$$

Hence, Eq. (8) can be written as.

$$\varphi_i = (\tau_1 (a_i + c_i) + \tau_2 \times b)\, \varphi_{max} \tag{10}$$

The brightness control can be achieved by varying the values of $a$, $b$, and $c$. Varying the $b$ levels will result in achieving 75% of dimming control without affecting the communication link, while varying both $a$ and $c$ levels will result in achieving the remaining 25% of dimming control. Since illuminance expresses the brightness of an illuminated surface, the illuminance level at a work place $j$ can be obtained by adding the illuminance form all the LED lamps. Hence, the total illuminance level $E_j$ can be expressed as [5], where $e_{ij}$ is the illuminance received at work place $j$ from a LED lamp $i$.

$$E_j = \sum_{i=1}^{I} e_{ij} \tag{11}$$

Assuming that the source has a Lambert radiation characteristics, $e_{ij}$ can be expressed as [5], where $m$ is the Lambert index, $d_o$ is the distance between the LED lamp and the photodiode (PD) receiver, $\theta$ is the angle of irradiance, and $\psi$ is the angle of incidence.

$$e_{ij} = \frac{(m + 1)\, \varphi_i}{2\pi d_o^2} \cos^m \theta \cos \psi \tag{12}$$

### C. NLOS CHANNEL MODEL

#### 1) COMMUNICATION

In an indoor environment, light has diffuse characteristics, which means that light undergoes multiple reflections between different surfaces within the room before reaching the receiver. Hence, the received power must extend to include the effect of both the LOS & NLOS components of the optical signal.

Since most reflections have diffuse nature, it is safe to assume that the interior materials and objects are purely diffusive [10]. A Lambertian radiation pattern as shown in Fig.3 for each element within the room can be assumed because the radiation pattern of an ideal diffuse reflector is independent from the incident light [30].

Under the assumption that the room surroundings (i.e. walls, floor, and ceiling) consists of small area segments $d_A$ that has Lambertian characteristics, the total optical

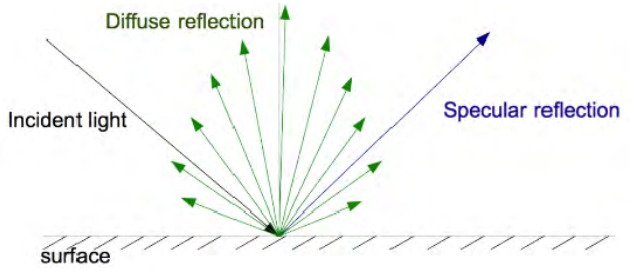


**FIGURE 3.** Diffuse and specular reflection.

power received from all the segments after $k$ bounces from a LED lamp can be expressed as [28], where $N_{ref}$ is the total number of reflections, $PL$ is the path-loss for each path, and $\Gamma_k$ represents the power of the reflected rays after $k$ bounces. While the integration is performed with respect to the surface $S$ of all the reflectors within the room.

$$P_{diffuse} = \left\{ \begin{matrix} \sum_{k=0}^{N_{ref}} \int_s (PL_1 PL_2 PL_3 \ldots PL_{k+1})\, \Gamma^k dA, & \theta_{k+1} \le FOV \\ 0, & \theta_{k+1} > FOV \end{matrix} \right\}, \quad k \ge 1 \tag{13}$$

where

$$\begin{aligned} PL_1 &= M_1 \times P^t_{max} \times \frac{A_{ref}(m+1)}{2\pi d_1^2} \cos^m \theta_1 \cos \psi_1, \\ PL_2 &= M_2 \times P^t_{max} \times \frac{A_{ref}(m+1)}{2\pi d_2^2} \cos^m \theta_2 \cos \psi_2, \\ PL_3 &= M_3 \times P^t_{max} \times \frac{A_{ref}(m+1)}{2\pi d_3^2} \cos^m \theta_3 \cos \psi_3, \\ &\vdots \\ PL_{k+1} &= M_{k+1} \times P^t_{max} \times \frac{A_{eff}(m+1)}{2\pi d_{k+1}^2} \cos^m \theta_{k+1} \cos \psi_{k+1} \end{aligned} \tag{14}$$

Hence, the total diffuse power can be expressed as follows.

$$P_{diffuse} = \left\{ \begin{matrix} \sum_{k=0}^{N_{ref}} M_k \times P^t_{max} \times \int_s (PL_1 PL_2 PL_3 \ldots PL_{k+1})\, \Gamma^k dA, \\ \quad \theta_{k+1} \le FOV \\ 0, \quad \theta_{k+1} > FOV \end{matrix} \right\}, \quad k \ge 1 \tag{15}$$

Thus, the total received power becomes.

$$P_r = P_j^r + P_{diffuse} \tag{16}$$

Therefore from equation (5), (15) and (16), the total received optical power can be expressed as.

$$P_j^r = \begin{cases} (c_i - a_i) \times P_{max}^t \times \dfrac{A_{eff}\,(m+1)}{2\pi d_o^2} T_s(\theta)\, g(\theta) \\ \quad \cos^m\theta \cos\psi, \quad \theta \le \text{FOV} \\ 0, \quad \theta > \text{FOV} \end{cases} + \begin{cases} \sum_{k=0}^{N_{ref}} M_k \times P_{max}^t \times \int_s (PL_1 PL_2 PL_3 \ldots PL_{k+1})\, \Gamma^k dA, \\ \quad \theta_{k+1} \le FOV \\ 0, \quad \theta_{k+1} > FOV \end{cases}, \quad k \ge 1 \tag{17}$$

From equation (16), the bit error rate for the proposed diffuse model $BER|_{diffuse}$ is given by.

$$BER|_{diffuse} = \frac{L/2}{L-1} Q\left(\frac{1}{2}\sqrt{\frac{3A_{eff}^2 L\,(P_r)^2 \log_2 L}{N_o R_b}}\right) \tag{18}$$

Hence, the minimum power required $P_{req}$, for a NLOS SC-LPPM scheme for achieving a given $BER|_{diffuse}$ is given by.

$$P_{req} = \frac{2}{A_{eff}} Q^{-1}\left(\left(\frac{L-1}{L/2}\right) \times BER|_{diffuse}\right) \sqrt{\frac{N_o R_b}{3L \log_2 L}} \tag{19}$$

By observing both Eqs. (14) and (15) with Fig. 4, one can conclude that, when taking the effect of multipath reflections, the received optical power is not directly proportional to the direct path length ($d_0$) only as in the LOS case. Instead, it also varies with other distances (i.e. $d_1$ to $d_{k+1}$), where $d_1$ is the distance between the LED and the first segment within the surroundings, and $d_{k+1}$ is the distance between the k$^{th}$ segment and the receiver (i.e. PD).

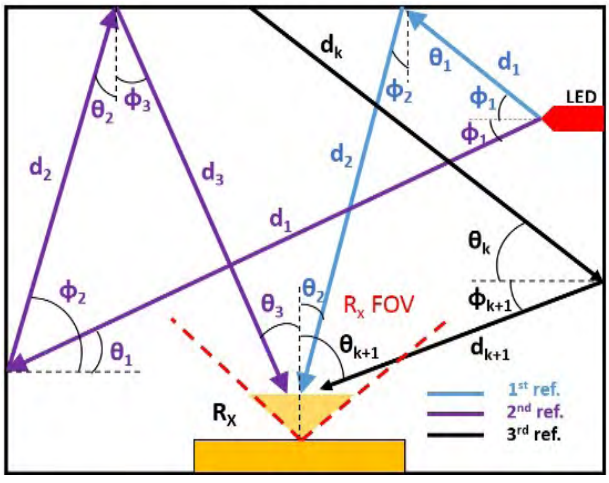


**FIGURE 4.** Structure of NLOS link.

### 2) ILLUMINATION

Based on the same assumption made in section II-C-1, that most reflections have diffuse nature, it is safe to assume that the interior materials and objects are purely diffusive with a Lambertian radiation pattern. Hence to evaluate the effect of the diffuse link on the system illumination performance, a model for NLOS illumination is presented in this section.

The received illumination from all the segments after $k$ bounces from a LED lamp can be expressed as, where, $I$ is the generated illumination by each reflector after $k$ bounces, and $\varphi_{ref}^k$ represents the output luminous flux generated by the walls after $k$ bounces.

$$E_{diffuse} = \sum_{k=0}^{N_{ref}} \frac{1}{2\pi} \int_s (I_1 I_2 I_3 \ldots I_{k+1})\, \varphi_{ref}^k dA, \quad k \ge 1 \tag{20}$$

where

$$\begin{aligned} I_1 &= \varphi_{max} \times \frac{(m+1)}{2\pi d_1^2} \cos^m\theta_1 \cos\psi_1, \\ I_2 &= \varphi_{max} \times \frac{(m+1)}{2\pi d_2^2} \cos^m\theta_2 \cos\psi_2, \\ I_3 &= \varphi_{max} \times \frac{(m+1)}{2\pi d_3^2} \cos^m\theta_3 \cos\psi_3, \\ &\vdots \\ I_{k+1} &= \varphi_{max} \times \frac{(m+1)}{2\pi d_{k+1}^2} \cos^m\theta_{k+1} \cos\psi_{k+1} \end{aligned} \tag{21}$$

Thus, the total received illumination becomes

$$E_r = \mathrm{E_j} + E_{diffuse} \tag{22}$$

Therefore from equation (11), (12), (20) and (22), the total received illumination can be expressed as

$$E_r = \sum_{i=1}^{I} \frac{(m+1)\,\varphi_i}{2\pi d_o^2} \cos^m\theta \cos\psi + \sum_{k=0}^{N_{ref}} \frac{1}{2\pi} \int_s (I_1 I_2 I_3 \ldots I_{k+1})\, \varphi_{ref}^k dA, \quad k \ge 1 \tag{23}$$

## D. SYSTEM DESIGN, PARAMETERS, AND SPECIFICATIONS

As mentioned in section II-A, there are four LED lamps that work together as an access point mounted at a height of 2.5 m within a (5×5×3 m$^3$) room. By taking a quadrant of the room (since the room and lighting geometry are symmetrical), the room corners are defined as (0.2 m×0.2 m) and the location under the light source is (1.25 m×1.25 m). Different LED parameters are listed in Table 1 to ensure both proper lighting and the communication process. Complementary room data with that mentioned in section II-A and information about the used receiver are also presented in Table 1.

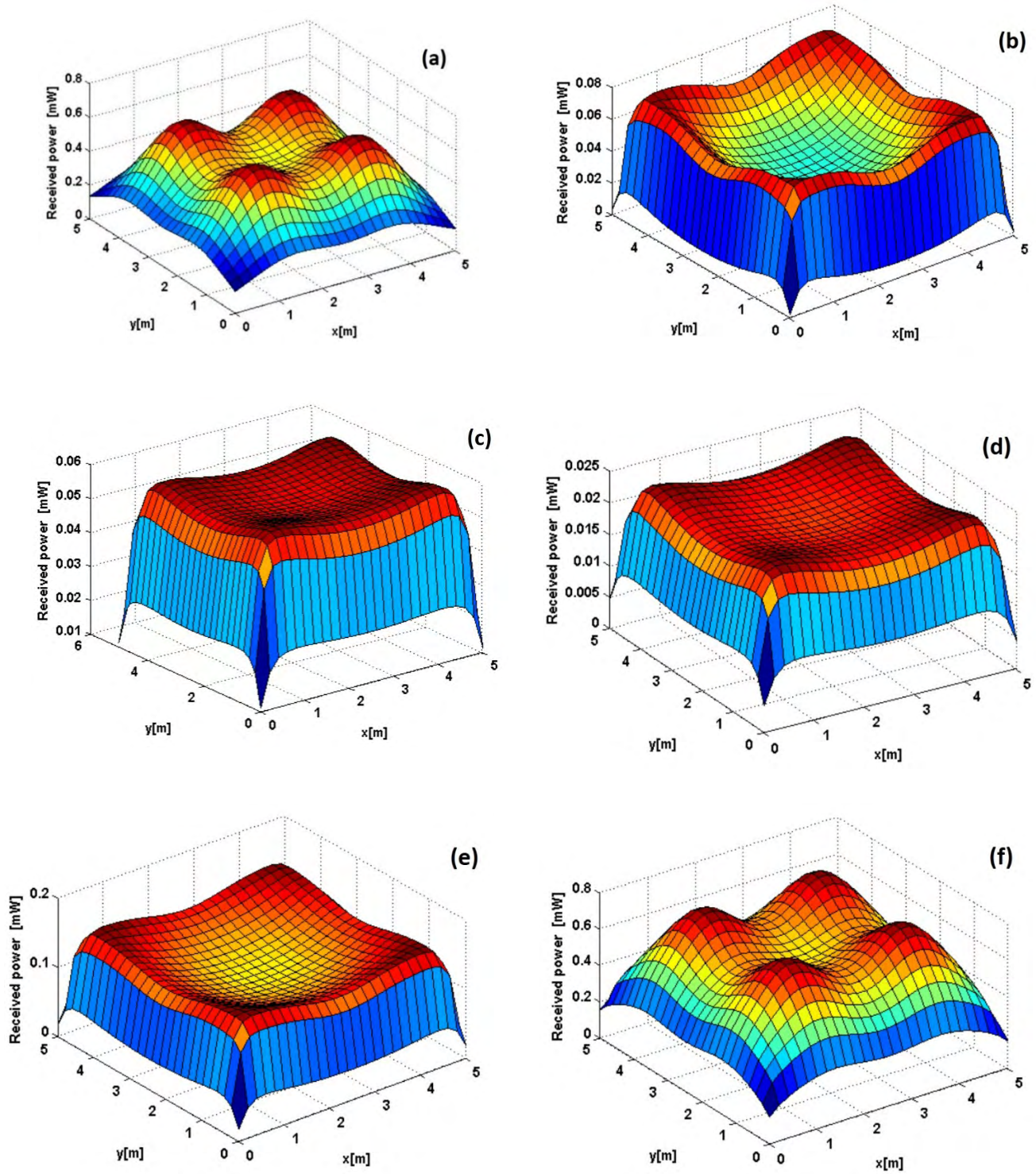


**FIGURE 5.** Received optical power due to (a) LOS path, (b) first reflection, (c) second reflection, (d) third reflection, (e) total diffuse power, and (f) overall link.

## III. PERFORMANCE EXPLORATION, EVALUATION, AND DISCUSSION

### A. INTRODUCTION

Exploring the power and illumination performance for NLOS SC-LPPM based VLC system and a comparison with LOS scenario is carried in section III-B. An investigation for the effect of different system/environmental parameters on the BER performance for both LOS/NLOS SC-LPPM VLC system scenarios is introduced section III-C.

It is noteworthy to mention that this work is based on the mathematical model that is presented in section II, meanwhile previous literatures investigated the performance

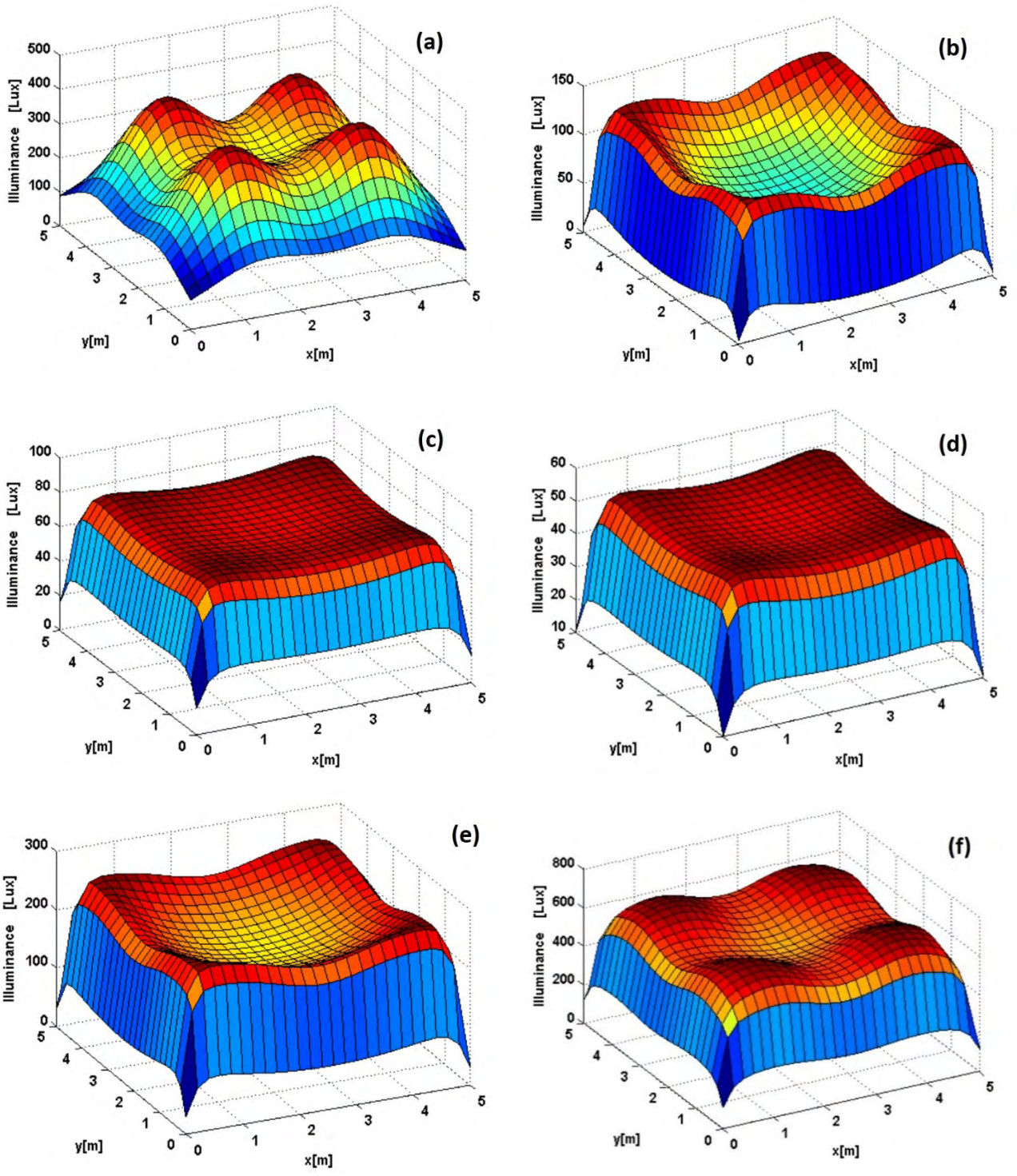


**FIGURE 6.** Received illumination due to (a) LOS path, (b) first reflection, (c) second reflection, (d) third reflection, (e) total diffuse power, and (f) overall link.

of other types of PPM schemes practically [31], [32]. In these studies, authors concluded that the practical system performance shows fair agreement with the theoretical analysis.

### *B. POWER AND ILLUMINATION DISTRIBUTION OF THE SYSTEM*

In this section, the received power and illumination distribution at desk level is discussed. Fig.5 and Fig.6 show the power

**TABLE 1. Simulation parameters.**

| | Parameters | Value |
|---|---|---|
| Room: | | |
| | Wall reflectivity | 0.8 |
| | Ceiling reflectivity | 0.5 |
| | Floor reflectivity | 0.2 |
| | Differential area | 0.2 x 0.2 $m^2$ |
| Source: | | |
| | Number of LEDs / LED lamp | 400 (20 x 20) |
| | LED transmitted power | 20 mW |
| | Semi-angle half power | 60° |
| | Center luminous intensity | 0.73 cd |
| | power spectrum density | $10^{-21}$ |
| Receiver: | | |
| | Area | 1 $cm^2$ |
| | Field of view (FOV) | 120° |
| | Responsivity | 0.4 A/W |
| | Concentrator refractive index | 1.5 |
| | Filter gain | 1 |

and illumination distribution within the proposed room topology for the LOS, 1st reflection, 2nd reflection, 3rd reflection, the total diffuse link distribution (i.e. summation of the 1st, 2nd, and 3rd reflection) and the overall link, respectively. It is noteworthy to mention that the overall link is the summation of the LOS component and the total diffuse link. The receiving surface is divided into 20 × 20 segments that form a grid that helps in calculating the power rating and illumination within the room.

As it can be observed from Fig.5 (a), the strongest LOS components are directly under the lighting sources and it decreases as the Rx moves towards the room corners to vary from 0.62 mW to 0.13 mW respectively. Another observation can be made from fig.5 (b, c, d, e) is that the reflection components maximized its contribution near the room walls, which compensates the decrease in the power levels in such area when compared to the LOS scenario. Taking the effect of all the NLOS components, i.e. Fig.5 (e) results in increasing the received power by 0.1547 mW at room corner and 0.1036 mW at room center.

When viewing the overall link, Fig 5 (f) shows that adding the NLOS component increases the total received power but still the LOS component dominates. The total received power is 0.74 mW under the light sources and 0.15 mW at the room corners.

As indicated in section I, SC-LPPM scheme can provide an acceptable illumination performance with a steady communication link. In the following part, and to the author best knowledge it is the first time to evaluate the illumination performance for a PPM based scheme under NLOS scenario.

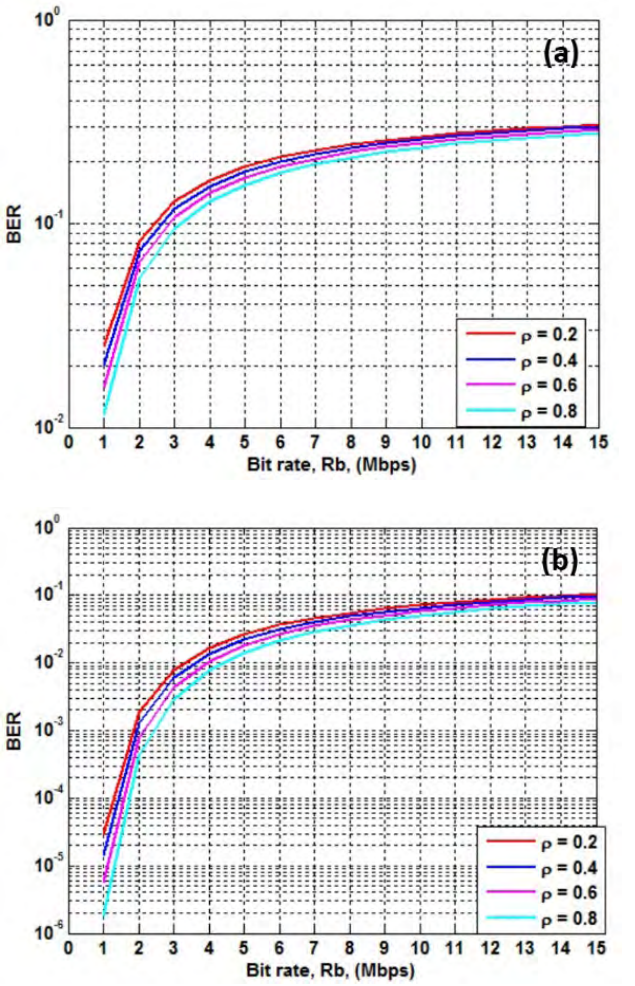


**FIGURE 7. BER vs. bit rate at different wall reflectivity for (a) L=2, (b) L=4.**

Analysis carried using the mathematical model introduced in section II-C-2.

Lighting performance is a prerequisite of SC-LPPM scheme. Hence, for an efficient system design, one must ensure that sufficient illumination is generated. In a typical room, it should be greater than 400 lux [5].

For LOS scenario, illumination decreases from 275 Lux under the light sources to 119 Lux at the room corners as indicated in Fig.6 (a). It is safe to conclude that within the presented room as the Rx locates between 1m × 1m will not meet the targeted illumination standard [5]. This is extracted from a quadrant of the room (since the room and lighting geometry are symmetrical).

Exploring the effect of including NLOS component that is shown in fig.6 (b, c, d, e), shows an enhancement in system's lighting performance as the illumination within the room increases especially at the room corners. It provides an extra illumination of about 260 lux at room corner and 175 lux at room center as indicated in Fig. 6 (e).

Therefore, one can conclude that adding the NLOS components will enhance the illumination performance to 433 Lux at the room corner and 665 Lux under the lighting source

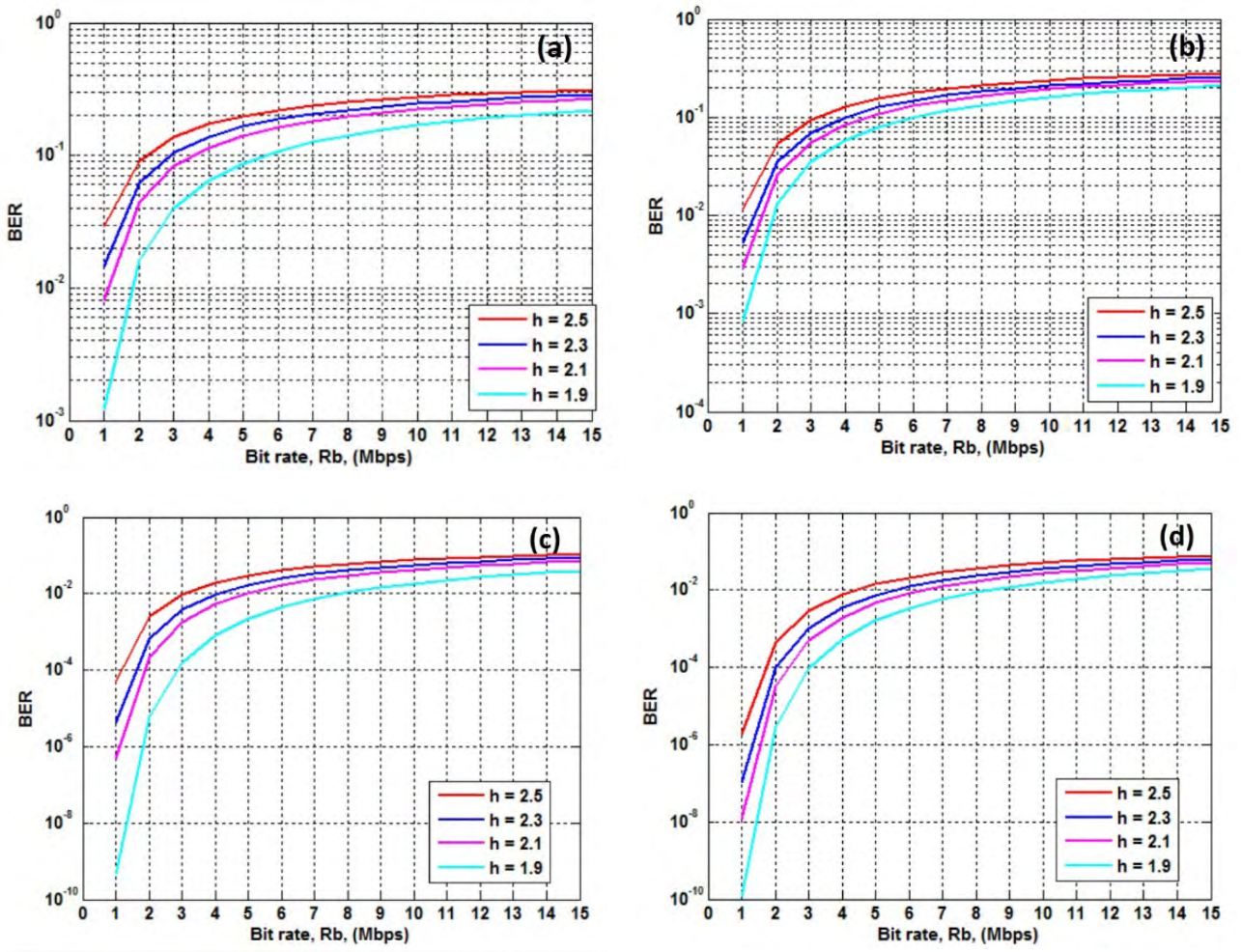


**FIGURE 8.** BER vs. bit rate at different Rx heights for (a) LOS scenario and L=2, (b) NLOS scenario and L=2, (c) LOS scenario and L=4, (d) NLOS scenario and L=4.

as indicated in fig.6 (f). Which meets sufficient illumination requirements and standards [5].

### C. EFFECT OF DIFFERENT SYSTEM/ENVIRONMENTAL PARAMETERS ON THE BER PERFORMANCE FOR BOTH LOS/NLOS

For an inclusive evaluation for the system performance, the effect of wall reflectivity, receiver (Rx) height, Tx semi-radiation angle, and different SCMF levels for both LOS/NLOS scenarios are presented respectively. The evaluation process also aims to explore the effect of these parameters on the BER performance at different operating system bitrates and modulation levels. Finally parameters, specifications and coordinates presented in section II-A and section II-D are used during this investigation.

#### 1) EFFECT OF WALL REFLECTIVITY

From fig.7, it can be observed that the system BER performance will improve as the wall reflectivity ($\rho$) increases. This results from the fact that more light rays will bounce off the walls resulting in increasing the total received power. This shows a fair agreement with the mathematical model equation (18). At 1 Mbps (i.e. relatively low VLC system bit rate), fig.7 (a) shows that for L=2 the BER varies from $2.5\times10^{-2}$ to $1.156\times10^{-2}$ for $\rho = 0.2$ and $\rho = 0.8$, respectively. While increasing the modulation level of the SC-LPPM scheme to L=4 will enhance the system performance to $2.9\times10^{-5}$ for $\rho = 0.2$, and $1.85\times10^{-6}$ for $\rho = 0.8$ as indicated in fig.7 (b).

For a higher bit rates (i.e. 15 Mbps), same behavior is observed with a much lower BER performance to reach approximately $(3.062\times10^{-1})$ for $\rho = 0.2$ and $(2.788\times10^{-1})$ for $\rho = 0.8$, at L=2, as indicated in Fig.7 (a), while for L=4 the BER performance is $(1.036\times10^{-1})$, $(8.028\times10^{-2})$ for $\rho = 0.2$ and $\rho = 0.8$, respectively as indicated in Fig. 7 (b).

#### 2) EFFECT OF RX HEIGHT

As shown in Fig. 8 (a, b, c, and d), the system BER performance enhances as the distance between the Tx and the Rx (h) decreases for both LOS and NLOS scenarios. Although such observation seems logical, this section provides an insight view about the following: 1) effect of different (L),

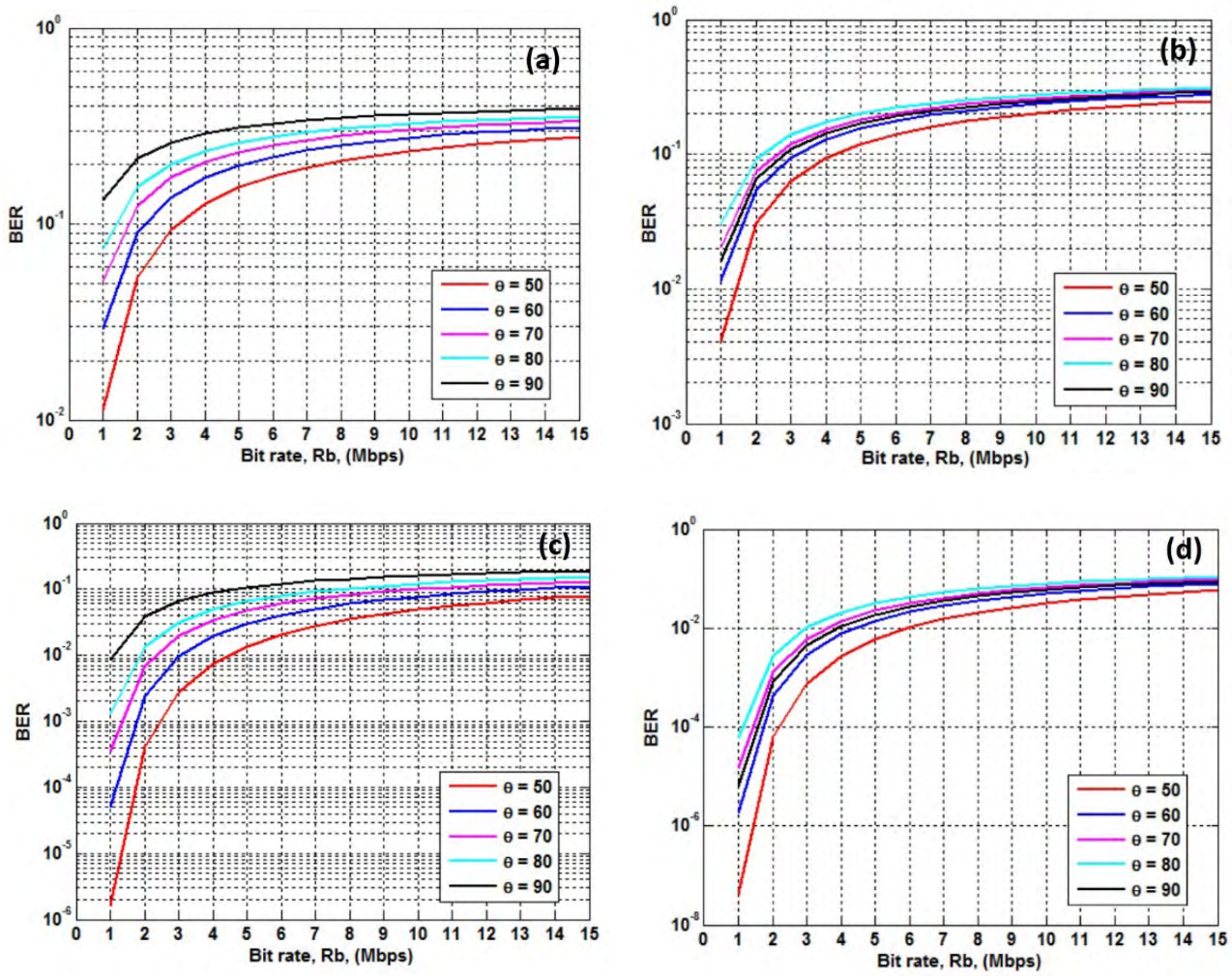


**FIGURE 9.** BER vs. bit rate at Tx semi-radiation angle ($\theta_{1/2}$) for (a) LOS scenario and L=2, (b) NLOS scenario and L=2, (c) LOS scenario and L=4, (d) NLOS scenario and L=4.

2) effect of the NLOS components, 3) high bitrate operation, and 4) effect of the incident angle ($\theta$).

It can be observed that the diffuse power will result in enhancing the system performance compared to the LOS system performance. Fig.8 (a, b) shows that at L=2 and 1 Mbps the system performance enhanced from $2.907\times10^{-2}$ to $1.212\times10^{-3}$ for LOS scenario and from $1.156\times10^{-2}$ to $8.357\times10^{-4}$ for NLOS scenarios at h=2.5m and h=1.9 m, respectively. Another observation can be made; increasing the modulation level to L=4 has a significant effect on the system performance as the BER enhances to $5.035\times10^{-5}$ and $8.78\times10^{-9}$ for LOS scenario and to $1.85\times10^{-6}$ and $9.04\times10^{-9}$ for NLOS scenarios at h=2.5 m and h=1.9 m, respectively as indicated in fig.8 (c, d).

For higher bitrates (i.e. 15 Mbps), the system BER performance becomes worse as it can be observed from Fig. 8, but it maintains the same behavior. At 15 Mbps, L=4, and by assuming an NLOS scenario the BER performance will decrease to $8.027\times10^{-2}$, $3.485\times10^{-2}$ for h=2.5, and h=1.9, respectively.

It is noteworthy to mention that, the previous discussion considers the effect of both the Rx height and the diffuse power at proper Rx location within the room as indicated in section II-A, and section II-D. However, at the room corners, it is noted that the system performance decreases as (h) decreases. This can be explained by noticing that the incidence angle ($\theta$) increases as the Rx height increases at the room corners, as it can be observed from (Fig. 4). Hence $A_{eff}$, of the Rx decreases, resulting in the noticeable decrease in the system BER performance.

### 3) EFFECT OF TX SEMI-RADIATION ANGLE ($\theta_{1/2}$)

Fig.9 shows the BER performance of the system through different Tx semi-radiation angle ($\theta_{1/2}$) for both LOS and NLOS scenarios. It can be observed from fig.9 (a, c) at 1 Mbps that for LOS scenario the system performance enhanced from $1.328\times10^{-1}$ (i.e. $\theta_{1/2}=90°$) to $1.12\times10^{-2}$ (i.e. $\theta_{1/2}=50°$) at L=2 and from $8.664\times10^{-3}$ (i.e. $\theta_{1/2}=90°$) to $1.65\times10^{-6}$ (i.e. $\theta_{1/2}=50°$) at L=4. Enhancing the system

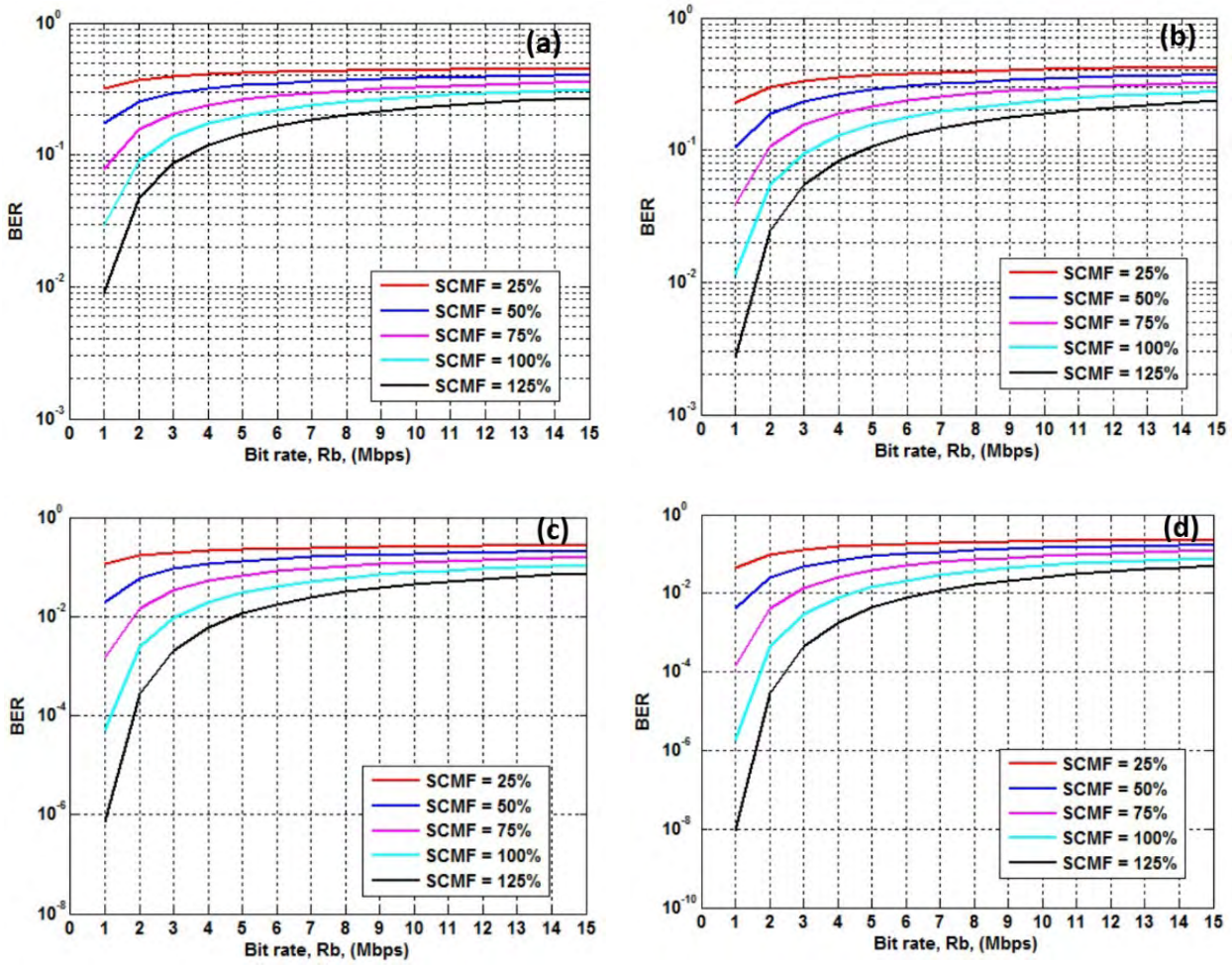


**FIGURE 10.** BER vs. bit rate at different SCMF for (a) LOS scenario and L=2, (b) NLOS scenario and L=2, (c) LOS scenario and L=4, (d) NLOS scenario and L=4.

BER performance when narrowing $\theta_{1/2}$ can be explained by observing that the Tx directivity increases as the angle minimizes. This results in increasing the received optical power collected from the distinct sources.

For the NLOS scenario, by operating with the same system rate and excluding $\theta_{1/2} = 90°$, fig.9 (b, d) shows similar behavior to LOS scenario as $\theta_{1/2}$ varies from 80° to 50° but with much improvement in the BER performance. An exception was observed at $\theta_{1/2} = 90°$ where the system performance shows a stunning improvement to beat the BER performance at $\theta_{1/2} = 70°$ and $\theta_{1/2} = 80°$ respectively.

An inverted behavior where the system performance enhances compared to LOS scenario. As $\theta_{1/2}$ varies from 50° to 90° to 0.03049 and $4.13\times10^{-3}$ at L=2 and to $5.955\times10^{-5}$ and $4.249\times10^{-8}$ at L=4, this comes from the nature of light reflections that accumulate with the increase of $\theta_{1/2}$.

For higher bit rates (i.e. 15 Mbps), the system performance becomes less efficient.

From the previous discussion and from fig.9; it can be assumed that at the room corners, higher values of $\theta_{1/2}$ will result in improving the system BER performance, as increasing $\theta_{1/2}$ will result in increasing the concentration area of the Tx which will enhance the BER performance at such location.

#### 4) EFFECT OF INCREASING THE SCMF

A performance analysis is performed to evaluate the effect of varying the SCMF of SC-LPPM scheme. In Fig 10, it is noteworthy to clarify that 25% of SCMF indicates that the system works in an extremely power saving mode with only 25% of the normal (i.e. moderate) LED power that is mentioned in Table 1 (25%*20mW = 5 mW/LED). Working at 100% SCMF indicates that system works at the designed value directly without modifications (i.e. 20 mW/LED).

From Fig.10 it can be shown that increasing the SCMF (from 25 % to 125%) results in enhancing the system BER performance for both LOS and NLOS scenarios due to the effect of the diffuse power.

Such improvement comes with a small price paid in system total power consumption which is the main advantage of such scheme. Once more, the increase of 25% in SCMF corresponds to a 5 mW increase per LED lamp, such increase

can be assumed as a low cost for increasing the system performance.

Fig.10 (a, b) shows that for LOS scenario the BER performance improved from $3.179\times10^{-1}$ to $8.934\times10^{-3}$ at L=2 and from 0.1145 to $7.242\times10^{-7}$ at L=4 as the SCMF varies from 25% to 125% respectively. While for NLOS scenario fig.10 (c, d) shows that the system performance improved from $2.269\times10^{-1}$ to $2.719\times10^{-3}$ at L=2 and from $4.71\times10^{-3}$ to $9.006\times10^{-9}$ at L=4 as the SCMF varies from 25% to 125% respectively.

## IV. CONCLUSION

This work explores the performance of SC-LPPM scheme in a diffuse (i.e. non-light-of-sight) environment. The power saving phenomena and relatively simple structure compared to other VLC modulation schemes make this investigation necessary.

Adding the NLOS components will enhance both the total received power and the lighting performance of the system. Several parameters can control and optimize the NLOS operation of the dimmable SC- LPPM scheme VLC system. Reflectivity, SCMF and L specifications will be nominated.

For diffuse scenario, a BER of $10^{-5}$ to $10^{-7}$ with L=4, normal wall reflectivity (plaster walls $\rho = 0.8$) and 100% SCMF (i.e. 20 mW/LED) can be achieved easily at bit rates of 1 to 2 Mbps. These BER performance levels can be enhanced by selecting wall painting/ materials with high reflectivity.

Narrowing the Tx semi-radiation angle ($\theta_{1/2}$) at L=4 and under the dispersive nature assumption will result in achieving a BER of $10^{-8}$.

As a power saving scheme, increasing SCMF with low power/LED level can enhance greatly the BER performance in the diffuse scenario. A remarkable value of $10^{-9}$ can be reached when increasing SCMF by 25% (i.e. to reach 25 mW/LED) under same conditions (L=4, $\rho = 0.8$ and 1-2 Mbps).

Unfortunately, at higher rates the performance is getting worse but still can be optimized and controlled through using a careful choice of environmental and system parameters that are provided through this work.

## REFERENCES

[1] A. Jovicic, J. Li, and T. Richardson, "Visible light communication: Opportunities, challenges and the path to market," *IEEE Commun. Mag.*, vol. 51, no. 12, pp. 26–32, Dec. 2013.
[2] D. O'Brien and M. Katz, "Optical wireless communications within fourth-generation wireless systems [invited]," *J. Opt. Netw.*, vol. 4, no. 6, pp. 312–322, 2005.
[3] L. Grobe *et al.*, "High-speed visible light communication systems," *IEEE Commun. Mag.*, vol. 51, no. 11, pp. 60–66, Dec. 2013.
[4] N. A. Mohammed and M. A. Elkarim, "Exploring the effect of diffuse reflection on indoor localization systems based on RSSI-VLC," *Opt. Express*, vol. 23, no. 16, pp. 20297–20313, Aug. 2015.
[5] I. Din and H. Kim, "Energy-efficient brightness control and data transmission for visible light communication," *IEEE Photon. Technol. Lett.*, vol. 26, no. 8, pp. 781–784, Apr. 15, 2014.
[6] C. Quintana, V. Guerra, J. Rufo, J. Rabadan, and R. Perez-Jimenez, "Reading lamp-based visible light communication system for in-flight entertainment," *IEEE Trans. Consum. Electron.*, vol. 59, no. 1, pp. 31–37, Feb. 2013.
[7] T. Yamazato *et al.*, "Image-sensor-based visible light communication for automotive applications," *IEEE Commun. Mag.*, vol. 52, no. 7, pp. 88–97, Jul. 2014.
[8] I. C. Rust and H. H. Asada, "A dual-use visible light approach to integrated communication and localization of underwater robots with application to non-destructive nuclear reactor inspection," in *Proc. IEEE Int. Conf. Robot. Automat. (ICRA)*, May 2012, pp. 2445–2450.
[9] C. G. Lee, *Visible Light Communication: Advanced Trends in Wireless Communication*. Paterson, NJ, USA: Intech, 2011.
[10] J. R. Barry, *Wireless Infrared Communications*. London, U.K.: Kluwer, 1994.
[11] C. G. Lee, *Visible Light Communication, Advanced Trends in Wireless Communication*. Paterson, NJ, USA: Mutamed Khalid, 2011.
[12] Y. Kozawa and H. Habuchi, "Enhancement of optical wireless multi-pulse PPM," in *Proc. IEEE Global Telecommun. Conf., (GLOBECOM)*, Dec. 2008, pp. 1–5.
[13] J. M. Kahn and J. R. Barry, "Wireless infrared communications," *Proc. IEEE*, vol. 85, no. 2, pp. 265–298, Feb. 1997.
[14] J. B. Carruther and J. M. Kahn, "Angle diversity for nondirected wireless infrared communication," *IEEE Trans. Commun.*, vol. 48, no. 6, pp. 960–969, Jun. 2000.
[15] J. G. Proakis, *Digital Communications*, 4th ed. New York, NY, USA: McGraw-Hill, 2000.
[16] B. Bai, Z. Xu, and Y. Fan, "Joint LED dimming and high capacity visible light communication by overlapping PPM," in *Proc. 19th Annu. Wireless Opt. Commun. Conf. (WOCC)*, May 2010, pp. 1–5.
[17] H. Sugiyama and K. Nosu, "MPPM: A method for improving the band-utilization efficiency in optical PPM," *J. Lightw. Technol.*, vol. 7, no. 3, pp. 465–472, Mar. 1989.
[18] S. Lou, C. Gong, N. Wu, and Z. Xu, "Joint dimming and communication design for visible light communication," *IEEE Commun. Lett.*, vol. 21, no. 5, pp. 1043–1046, May 2017.
[19] T. Ohtsuki, I. Sasase, and S. Mori, "Overlapping multi-pulse pulse position modulation in optical direct detection channel," in *Proc. IEEE Int. Conf. Commun. (ICC)*, vol. 2, May 1993, pp. 1123–1127.
[20] A. Chizari, M. V. Jamali, S. Abdollahramezani, J. A. Salehi, and A. Dargahi, "Visible light for communication, indoor positioning, and dimmable illumination: A system design based on overlapping pulse position modulation," *Optik*, vol. 151, pp. 110–122, Dec. 2017.
[21] D. Shiu and J. M. Kahn, "Differential pulse-position modulation for power-efficient optical communication," *IEEE Trans. Commun.*, vol. 47, no. 8, pp. 1201–1210, Aug. 1999.
[22] M. Noshad and M. Brandt-Pearce, "Expurgated PPM using symmetric balanced incomplete block designs," *IEEE Commun. Lett.*, vol. 16, no. 7, pp. 968–971, Jul. 2012.
[23] M. Noshad and M. Brandt-Pearce, "Application of expurgated PPM to indoor visible light communications—Part I: Single-user systems," *J. Lightw. Technol.*, vol. 32, no. 5, pp. 875–882, Mar. 1, 2014.
[24] M. Noshad and M. Brandt-Pearce, "Multilevel pulse-position modulation based on balanced incomplete block designs," in *Proc. Global Commun. Conf. (GLOBECOM)*, Dec. 2012, pp. 2930–2935.
[25] *IEEE Standard for Local and Metropolitan Area Networks—Part 15.7: Short-Range Wireless Optical Communication Using Visible Light*, Institute of Electrical and Electronics Engineers, Standard 802.15.7-2011, Sep. 2011.
[26] H. Sugiyama, S. Haruyama, and M. Nakagawa, "Brightness control methods for illumination and visible-light communication systems," in *Proc. 3rd Int. Conf. Wireless Mobile Commun.*, Mar. 2007, p. 78.
[27] D. Deqiang, K. Xizheng, and X. Linpeng, "An optimal lights layout scheme for visible-light communication system," in *Proc. 8th Int. Conf. Electron. Meas. Instrum. (ICEMI)*, Aug. 2007, pp. 2-189–2-194.
[28] K. Lee, H. Park, and J. R. Barry, "Indoor channel characteristics for visible light communications," *IEEE Commun. Lett.*, vol. 15, no. 2, pp. 217–219, Feb. 2011.
[29] C. Sertthin, "An indoor positioning architecture based on visible light communication and multiband received signal strength fingerprinting," Graduate School Sci. Technol., Keio Univ., Tokyo, Japan, Tech. Rep., 2011.
[30] T. Komine, J. H. Lee, S. Haruyama, and M. Nakagawa, "Adaptive equalization system for visible light wireless communication utilizing multiple white LED lighting equipment," *IEEE Trans. Wireless Commun.*, vol. 8, no. 6, pp. 2892–2900, Jun. 2009.
[31] L. Mao, C. Li, H. Li, X. Chen, X. Mao, and H. Chen, "A mixed-interval multi-pulse position modulation scheme for real-time visible light communication system," *Opt. Commun.*, vol. 402, pp. 330–335, Nov. 2017.
[32] N. Kumar, "Visible light communication system for road safety applications," Ph.D. dissertation, Dept. Elect. Eng., Aveiro Univ., Porto, Portugal, 2011.

**NAZMI A. MOHAMMED** received the Ph.D. degree in wireless optical communications from Alexandria University, Egypt, in 2010. He is currently a part-time Associate Professor at the Electronics and Communication Engineering Department, Obour Institutes, Obour City, Egypt. He has authored and co-authored over 40 journal and conference papers and has supervised over 15 M.Sc. and Ph.D. graduate students. His current research interests include optical communications, optoelectronics, and photonics.

**KAREEM A. BADAWI** received the B.S. degree in electronics and communications engineering from the Higher Technological Institute, Cairo, Egypt, in 2010, and the M.Sc. degree from the Arab Academy for Science, Technology and Maritime Transport, Alexandria, Egypt, in 2016. He is currently an Instructor at the Electronics and Communication Engineering Department, Higher Technological Institute, Egypt. His current research interests include free space optical communication and visible light communication (Li-Fi).